Spring 2020

Production of Entangled Photons via Spontaneous Parametric Down-Conversion

Logan P. Kaelbling
Bard College, ek4680@bard.edu

Production of Entangled Photons via Spontaneous Parametric Down-Conversion

A Senior Project submitted to
The Division of Science, Mathematics, and Computing
of
Bard College

by
Logan Kaelbling

Annandale-on-Hudson, New York
May, 2020

Abstract

Quantum entanglement, a phenomenon in which the behavior of one particle is somehow immediately correlated with and informed by what is happening to a partner particle a long distance away, has been a pivotal part of the formulation of quantum theory as we know it today and is currently generating many promising avenues of research. As such, finding ways to reliably and inexpensively generate systems of entangled particles for research purposes has become crucial. For my project, I attempt to set up a system that generates energy- and polarization-entangled photons via a technique called spontaneous parametric down conversion. This method for generating entangled particles involves shooting a laser beam at a special type of nonlinear crystal. Most of the photons in the beam pass right through the crystal, but some are absorbed by it. An absorbed photon's energy excites the crystal, which then releases that energy by emitting a pair of entangled photons. This occurs tens of thousands of times per second to create two streams of photons where each photon in one beam has an energy-entangled partner in the other. These photons can then be manipulated and employed in experimental examinations of a variety of quantum optical phenomena.

Contents

Dedication

Even though it's cliché, I have to dedicate this thesis to my parents Leslie and David Kaelbling, and to Tina Delorey. They have loved and supported me for my entire life and I wouldn't be here without them. I hope to continue to grow and learn and make them proud of the person they have raised.

Acknowledgments

I would like to acknowledge and thank all of the math and physics professors who have been so kind and patient with me during my time at Bard. I would especially like to thank Associate Dean Timand Bates and my advisor, Antonios Kontos, because I owe the existence of this thesis in no small part to their enduring support and faith in my abilities.

1
Introduction

1.1 A Brief Introduction to Quantum Theory

The theory of quantum mechanics is based on the idea that any particle (be it light or matter) can be associated with a wave function that fully describes it. This wave function is informed by the particle's environment. Different mathematical operators can be applied to a wave function to get information about the particle, such as its energy, momentum, and spin. In its natural state, when it is not observed, the information the wave function contains is not what we would expect from classical mechanics. For example, if I apply the momentum operator to a particle's wave function in an attempt to find out its momentum, the result will not be a definite value, but a set of all the different possible momenta and the probability of finding each one when I actually measure the particle's momentum. Each possible momentum value is called a momentum eigenvalue, and by applying the momentum operator to the wave function, we have expressed the wave function as a sum of the different momentum eigenstates multiplied by their respective probabilities without changing it or losing any information. Then the only case in which looking at a wave function will give us a definite value for the momentum of the particle is when that wave function is already one of its eigenstates, and as such applying the momentum operator gives us a single term with 100% certainty.

If in almost all situations the wave function can only give us a set of possibilities, one might think this means that it just doesn't contain all of the information- if it did, shouldn't it be able to tell us which momentum the particle is actually experiencing? But quantum mechanics says instead that the wave function does know everything, and it is not a question of knowing which situation is correct because the particle is not actually experiencing any single one of them. Until we actually measure the particle's momentum, it does not have a definite momentum. When we do measure the momentum, the particle 'picks' one of the different possible momenta; the act of measuring the particle's momentum collapses its wave function into one of the momentum eigenstates.

This collapse fundamentally changes the wave function- and therefore also fundamentally changes the particle. Any information we had about the particle before measurement is no longer relevant, because a new wave function means new results when the different operators are applied. This can be beneficial in that once we measure a certain attribute of a particle, we know with certainty what its wave function is, so we can do specific measurements to prepare particles in specific states. However, in doing so, we also destroy any information to be found about the particle's previous state. Observing a particle is not a passive act, and the significance of observation, measurement, and uncertainty lie at the heart of quantum theory.

1.2 The Einstein-Podolsky-Rosen Paradox

The inherent indeterminism of quantum theory unsettled Einstein. In a 1926 letter to fellow physicist Max Born, he famously objected that "I, at any rate, am convinced that God does not play dice with the universe." Nine years later, he published a paper with physicists Boris Podolsky and Nathan Rosen called "Can Quantum-Mechanical Description of Physical Reality be Considered Complete?" [2] in which they presented a formal objection to quantum theory by way of a thought experiment now known as the EPR paradox. It begins with the consideration of a particle's behavior in one dimension.

First they prove that, according to the current formulation of quantum mechanics, "when the momentum of a particle is known, its position has no physical reality". Given the laws of quantum mechanics, it is impossible for one to know the particle's position and its momentum at the same time. This is because having a definite position means its wave-function is a position eigenstate, but position eigenstates are not the same as momentum eigenstates, and an attempt to probe the momentum of a wavefunction in a position eigenstate by applying the momentum operator to it can only ever yield a superposition of multiple momentum eigenstates. If we try to measure the momentum directly instead, the particle's wave function will collapse into a momentum eigenstate, and as such will no longer have a definite position. The EPR paper's proof of this follows along these lines by providing a general form of a particle in a momentum eigenstate, applying the position operator to this wavefunction, and demonstrating that, in the position basis, the momentum eigenstate becomes a superposition of an infinite number of equally likely position states, which means the particle could be anywhere in space with equal probability. (This language is slightly misleading in that it implies that the particle can have a singular position- the closest we can come theoretically is knowing with certainty that the particle is within a specified region, and then squeezing that region down to be infinitesimal; experimentally, position (and all other) measurements are limited by the precision of our instruments and as such any measurement comes with a margin of error, so again we have a band of possible values and not one specific point).

Having established that assuming quantum mechanics is complete and a particle's wave function fully describes it implies that a particle cannot have a definite momentum and position (or any other two observable quantities whose eigenstates are not compatible) at the same time, the authors describe a system that appears to contradict this which, although they did not have the term for it at the time, is built upon the principle of quantum entanglement. Entanglement is a phenomenon where two (or more) particles are generated together or interact in such a way that their wave functions are dependent upon each other. This dependency can be in one of many different observable quantities. For instance, when two particles are position-entangled, finding

the position of one particle tells you with certainty what the position of the other particle is without ever actually observing it. The EPR paper points out that this leaves you free to perform a momentum measurement on the second, undisturbed particle and as such, if only for an instant, one can know definite values for both its position and momentum, which according to quantum theory should be impossible. They go on to point out that the 'reality' of the second particle (which of its observables has a definite value) will "...depend upon the process of measurement carried out on the first system, which does not interact with the second system in any way. No reasonable definition of reality could be expected to permit this." This has been pretty well-confirmed to be the case, and so I suppose our reality must be unreasonable.

At first Einstein suggested that there must be more going on. He thought that there must be some communication happening between the particles that was not encoded in their wave functions that could explain this correlation and provide causality to the seemingly-uncertain and probabilistic nature of quantum measurement which he called hidden variables. However, it's Einstein's work on relativity that tells us that nothing, even information, can travel faster than the speed of light. Experiments have been done in which a pair of entangled particles are separated very far apart and measurements are done on both simultaneously, so that there was not enough time for the particles to 'coordinate' their results even at light speed, and still the particles' outcomes were complimentary in every case without, when considered individually, any change in their quantum behavior or any indication of more 'certainty' than any other, non-entangled quantum particle.

1.3 Bell's Theorem

This kind of experiment was a precursor to what are known as Bell experiments, based off of John Bell's 1964 response to the EPR paper called "On the Einstein Podolsky Rosen Paradox"[3]. In the original thought experiment, Bell considers the correlation between spin measurements done at different axes on a pair of spin-entangled particles. A spin measurement has a binary outcome, meaning it will always result in either 'up' or 'down'. Then the amount of correlation

between the two particles' spins is found by adding 1 each time the spins are found to match and subtracting one each time they are opposite, and then dividing by the number of trials to find the average likelihood that the two will match. If we measure their spins on the same axis, the spins are always anti-correlated, which corresponds to a correlation of -1. If their spins are measured on anti-parallel axes (meaning there is an angle of 180 degrees between the measurement axes of the two particles), the resulting spins will always match, corresponding to a correlation of 1. If the two particles' spins are not correlated, then each time a measurement is done on both of them, there is a 50/50 chance that their spins will match. This means as long as we do enough trials for the results to be statistically significant, we'll get roughly the same number of instances of matching spins as opposing spins and the resultant correlation factor will be approximately 0. There are different operators for predicting spin values in each of the three spatial dimensions, and these operators do not commute, which means that knowing a particle's spin along one axis precludes definitive knowledge of its spin along any perpendicular axis. Then if we measure the first entangled particle along, say, the x-axis, both particles' wave functions will collapse into eigenstates of the x-spin operator. Then we try to measure the y-spin of the second particle, but because it is in an x-spin eigenstate, we know from applying the y-spin operator to its wave function that there's a 50/50 chance of measuring each possible spin along the y-axis, indicating that they are not at all correlated. This means that when there is a 90 degree angle between the axes of measurement for our two entangled particles, we should get an average correlation of 0 between the two spins.

Bell considers the change in correlation affected by increasing the angle between the measurement axes of the particles both from a classical viewpoint and from a quantum one, given the necessary points described by the situation above (correlation is -1 when the angle is 0 degrees, 0 at 90 or 270 degrees, and 1 at 180 degrees). According to classical mechanics, the change in correlation should be linear (meaning the correlation varies directly with the change in angle), while quantum mechanics tells us that for small angles, the change in correlation should vary with the square of the change in angle. If we start with the axes perpendicular (at 90 degrees

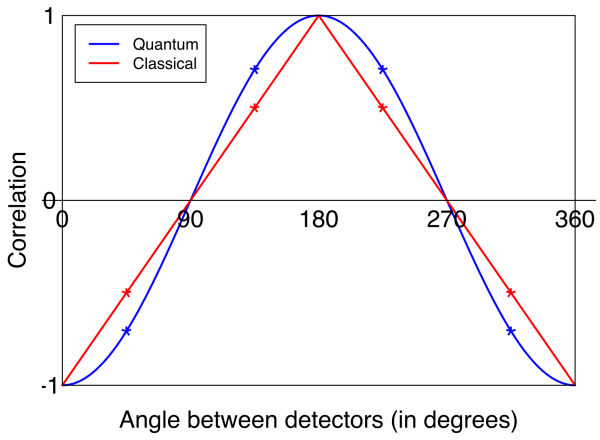

Figure 1.3.1. A graph of expected correlation as a function of angle

to each other), we're expecting a correlation of 0. Then when we add a few degrees to change the angle, both regimes say that the correlation will begin to increase, but they disagree about the rate at which this will occur. If we double the change in angle, quantum mechanics predicts a four-fold increase in correlation, while classical mechanics would expect it to double. Bell's inequality places a bound on the amount of correlation possible between two particles according to classical mechanics. At all the intermediate angles, one can see that the quantum prediction for correlation is not equal to the classical one. By examining the amount of correlation between the two particles' spins at specific angles (generally the angles with the greatest discrepancy between the classical and quantum predictions, which are marked on Fig. 1.3.1), we can see whether the correlation exceeds the bound put upon it by Bell's inequality. Then we should be able to tell whether the particles are behaving in accordance with classical mechanics, which would bolster the argument for hidden variables and the incompleteness of quantum theory, or in accordance with quantum mechanics. Bell experiments are still done to this day, and all of them have supported the predictions of quantum mechanics, but this experiment and its implications are full of philosophical subtleties and critics continue to point out possible 'loopholes' in the procedure that prevent it from definitively disproving Einstein's theories on local realism.

However, the overwhelming data supporting the quantum formulation has led to the theories of hidden variables and local realism falling out of favor with almost all physicists, and it is generally considered to be true that a particle's wave function contains absolutely all of its knowable information.

Entanglement has been a pivotal part of the formulation of quantum theory as we know it today and is currently generating many promising avenues of research. As such, finding ways to reliably and inexpensively generate systems of entangled particles for research purposes has become crucial. For my project, I attempted to set up a system that generates energy- and/or polarization-entangled photons via a technique called spontaneous parametric down conversion. This method for generating entangled particles involves shooting a laser beam at a special type of nonlinear crystal. Most of the photons in the beam pass right through the crystal, but some are absorbed by it. An absorbed photon's energy excites the crystal, which then releases that energy by emitting a pair of entangled photons. This occurs tens of thousands of times per second to create two streams of photons where each photon in one beam has an energy-entangled partner in the other. These photons can then be manipulated and employed in experimental examinations of a variety of quantum optical phenomena.

In the following chapters I will explain some of the quantum theory underlying this experiment, go over the experimental equipment and procedure, and propose future directions for the project to take.

2
Theory of Photon Pair Down-Conversion

2.1 Spontaneous Parametric Down-Conversion

Spontaneous parametric down-conversion is the method by which entangled photons will be generated. In this process, a laser beam is directed at a crystal. While most of the photons will pass through the crystal unaffected, sometimes the crystal will absorb the photon and release two down-converted photons in its place. This process can be used to generate single photons or entangled pairs of photons with specific wavelengths. The label 'parametric' means that the process occurs instantly and without changing the quantum state of the crystal, thus preserving the laws of conservation of energy and momentum, which dictate the necessary structure of the experimental set-up upon application to the photons involved.

2.1.1 Light in a Medium

When light travels through a medium as opposed to vacuum, its frequency ν remains unchanged but its phase velocity v and wavelength λ decrease in proportion to the medium's index of refraction r, which is calculated empirically and can be dependent on the crystal temperature, the incoming photons' wavelength and/or incident angle with the medium, and in the case of birefringent materials, the light's polarization. As a result of the change in velocity upon entering a new medium, the light is refracted and the direction of propagation changes according to Snell's

Law, which states that $n_1 \sin(\theta_1) = n_2 \sin(\theta_2)$, where θ_1 is the angle between the incident light beam and the vector perpendicular to the face of the medium, and θ_2 is the angle between refracted beam in the material and the same vector. The changes in velocity and frequency for light travelling vacuum to a medium are given by

$$v = \frac{c}{n} \tag{2.1.1}$$

where $c \approx 3 * 10^8 \text{m/s}$ is the speed of light in vacuum and v is the speed of light in a medium with refractive index n, and

$$n * \lambda' = \lambda \tag{2.1.2}$$

where λ' is the light's wavelength in the medium.

2.1.2 Light Polarization

Light is often thought of as a wave that wiggles up and down in space, and as such a light wave has two directions associated with it. The first is the direction of propagation, described by the wave vector, which points in the direction the light is travelling. The second is the polarization, which points in the direction along which the electric field is oscillating as the wave travels, or propagates, through space. The polarization is always perpendicular to the direction of propagation, but this leaves a whole two-dimensional plane of possible directions. For example, if the light wave is traveling in the x-direction, then it could be vertically polarized (polarized in the z-direction), or it could be horizontally polarized (polarized in the y-direction), or it could point in any direction in between these in the yz plane.

2.1.3 Conservation of Energy

In order for energy to be conserved, the total energy of the system must be the same before and after the down-conversion process. This means that the energy of the pumped photon (E_0) must be equal to the sum of the energies of the down-converted photons (E_1 and E_2). Expressed mathematically, this means that

$$E_0 = E_1 + E_2 \tag{2.1.3}$$

The Planck-Einstein relation tells us that the energy of a photon is given by $E = h\nu$, where $h \approx 6.6 * 10^{-34}$J*s is Planck's constant. Equation 2.1.1 and the fact that $v = \nu\lambda'$ tells us that $\nu = \frac{c}{n\lambda'}$. From Equation 2.1.2 this means $\nu = \frac{c}{\lambda}$, and plugging this into the Planck-Einstein relation for energy, Equation 2.1.3 becomes

$$\frac{1}{\lambda_0} = \frac{1}{\lambda_1} + \frac{1}{\lambda_2} \tag{2.1.4}$$

This is the restriction implicated by conservation of energy on the possible combinations of wavelengths that will be effective for down-conversion.

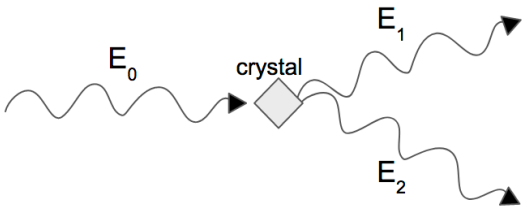

Figure 2.1.1. The pump photon's energy E_0 is absorbed by the crystal and then emitted as two photons with energies E_1 and E_2

2.1.4 Conservation of Momentum

Conservation of momentum applied to the process of spontaneous parametric down-conversion tells us that

$$\vec{p_0} = \vec{p_1} + \vec{p_2} \tag{2.1.5}$$

The momentum of a photon is proportional to its wave vector $\vec{k} = \frac{2\pi}{\lambda}\hat{k}$, where $\hat{k}$ points in the direction of propagation of the wave, and is given by $\vec{p} = \hbar\vec{k} = \frac{hn}{\lambda'}\hat{k}$. We choose our axes such that $\hat{p_0} = \hat{x}$, and $\vec{p_1}$ and $\vec{p_2}$ are perpendicular to $\hat{z}$. Then $\vec{p_0} = \frac{n_0 h}{\lambda_0'}\hat{x}$, $\vec{p_1} = \frac{n_1 h \cos\theta_1}{\lambda_1'}\hat{x} + \frac{n_1 h \sin\theta_1}{\lambda_1'}\hat{y}$, and $\vec{p_2} = \frac{n_2 h \cos\theta_2}{\lambda_2'}\hat{x} + \frac{n_2 h \sin\theta_2}{\lambda_2'}\hat{y}$, where θ_1 is the angle between $\hat{p_1}$ and $\hat{x}$, and θ_2 is the angle between $\hat{p_2}$ and $\hat{x}$. Applying Equation 2.1.5 component-wise and cancelling out Planck's constants yields two expressions that embody conservation of energy during down-conversion in the x- and y-direction respectively:

$$\frac{n_0}{\lambda_0'} = \frac{n_1 \cos\theta_1}{\lambda_1'} + \frac{n_2 \cos\theta_2}{\lambda_2'} \tag{2.1.6}$$

and

$$\frac{n_1 \sin\theta_1}{\lambda_1'} + \frac{n_2 \sin\theta_2}{\lambda_2'} = 0 \tag{2.1.7}$$

2.1.5 Birefringent Media

In order for the process to work properly for generating entangled photons, it is necessary that the output photons have the same wavelength and, in the case of type-1 SPDC, this means that they will experience the same refractive indices as well. Applying these new restrictions ($n_1 = n_2$ and $\lambda_1 = \lambda_2$) to Equations 2.1.4 and 2.1.6 respectively, we are left with the restrictions on SPDC in their final form:

$$\lambda_1 = \lambda_2 = 2\lambda_0 \tag{2.1.8}$$

and

$$n_0 = n_1 \cos\theta_1 = n_2 \cos\theta_2 \tag{2.1.9}$$

Equations 2.17, 2.1.8, and 2.1.9 constitute a system of three equations. If we impose the restriction that the pump beam's index of refraction must equal to the down-converted photons' index of refraction, then there is no way to solve this system of equations if index of refraction is really only dependent on wavelength. This means that we need a special material in which the indices of refraction depend on something other than wavelength, on some parameter that's not the same for both beams. Luckily for us, there is a whole class of media for which the index of refraction of incident light is dependent upon the light wave's polarization and propagation direction, known as birefringent media. Birefringent crystals have an extraordinary index of refraction along their optical axis, and two ordinary indices of refraction along axes perpendicular to the optical axis and to each other. In a uniaxial birefringent medium such as the one we will use, the two ordinary indices are the same. The generated photons will have a polarization perpendicular to that of the pump beam, which allows them to have different indices of refraction.

The relation between the incident light angle α and the ordinary and extraordinary indices in a uniaxial birefringent crystal is given by

$$\frac{\cos^2\alpha}{n_o} + \frac{\sin^2\alpha}{n_e} = [n_o \cos\sin^{-1}\frac{n_{air}\sin\theta_1'}{n_o}]^{-2} \tag{2.1.10}$$

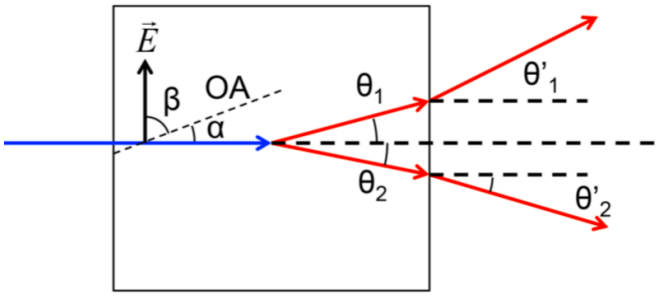

Figure 2.1.2. this diagram illustrates where β is, relates the crystal's optical axis to the photons' polarizations, and shows how each photon refracts and propagates through the crystal

Our crystal will be mounted with its optical axis at an angle α with the waves' propagation direction (which will from now on be defined as the $\hat{x}$ direction) in the xz-plane. Then if the pump beam is polarized in the $\hat{z}$ direction, its polarization will form an angle $\beta = \frac{\pi}{2} - \alpha$ with the optical axis and produce photons polarized in the $\hat{y}$ direction. Because their polarization is in the $\hat{y}$ direction but the optical axis lies in the xz-plane and is therefore perpendicular to $\hat{y}$ regardless of the value of β, the generated photons will experience the ordinary index of refraction, so $n_1 = n_o$. If the optical axis pointed in the $\hat{z}$-direction (meaning $\beta = 0$), then we would have $n_0 = n_e$. This is a step in the right direction, but finding a material that has ordinary and extraordinary indices of refraction such that $n_e(\lambda_0) = n_o(2 * \lambda_0)$ for any pump beam wavelength λ_0 will be a challenge, not to mention one that will work at a convenient wavelength. However, by increasing β, we decrease the component of the pump beam polarization that is parallel to the extraordinary axis and change the index of refraction experienced by the pump beam while the optical axis remains perpendicular to the down-converted photons' polarization and thus the index of refraction they experience remains unchanged. Then n_0 is a superposition of n_o and n_e with magnitudes $\cos(\alpha)$ and $\sin(\alpha)$ respectively, so the relationship between the modified n_0 and α is given by the equation

$$n_0 = (\frac{\cos^2\alpha}{n_o^2} + \frac{\sin^2\alpha}{n_e^2})^{-\frac{1}{2}}$$

This means we can take a wide range of media and pump wavelengths, and use this relation to adjust β and tune $n_0(\lambda_0)$ so that $n_0(\lambda_0) = n_1(\lambda_1) = n_o(2 * \lambda_0)$, thus satisfying Equations 2.1.8 and 2.1.9.

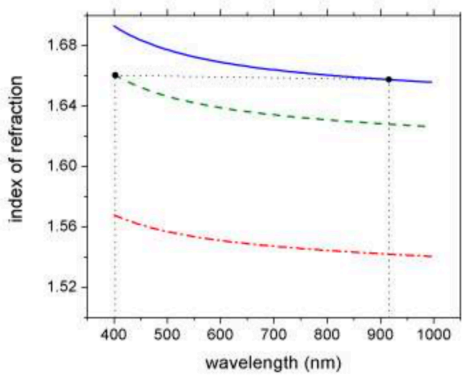

Figure 2.1.3. The blue line shows the ordinary index of refraction for a BBO crystal as a function of wavelength. The red dashed line is the extraordinary index of refraction for BBO, and the green dashed line is the modified extraordinary index of refraction when $\beta = 29$ degrees. The BBO's modified extraordinary index of refraction at approximately 405nm, which is the index of refraction felt by the pump photon, is roughly equivalent to BBO's ordinary index of refraction at 810nm.

We employ a crystal commonly used for SPDC, a Beta Barium-Borate, or BBO crystal (β-BaB_2O_4). If we're planning to use a 405nm pump beam on this crystal (and it just so happens we are), then unfortunately $n_e(\lambda_0) \neq n_o(2 * \lambda_0)$ and using the crystal with the optical axis in the $\hat{z}$ direction will not satisfy our constraints. However, if we tilt the optical axis back so that $\beta = 29$ degrees, its ordinary and modified extraordinary refractive indices are given by

$$n_e(\lambda) = [2.7359 + \frac{0.01878}{\lambda^2 - 0.01667} - 0.0134\lambda^2]^{\frac{1}{2}}$$

and

$$n_o(\lambda) = [2.3753 + \frac{0.01224}{\lambda^2 - 0.01667} - 0.01516\lambda^2]^{\frac{1}{2}}$$

with λ expressed in μm, and everything works out!

2.1.6 Type-II SPDC

In section 2.1.2, we chose our y-axis arbitrarily to simplify the conservation of momentum calculation. The rotational symmetry in the zy-plane means that the emitted beams can come anywhere along a cone whose radius is (due to the refractive index's dependence on wavelength)

determined by the beam's wavelength. In order to be entangled, the two emitted photons must be indistinguishable. This can be achieved in two different ways, with two identical, very thin birefringent crystals with the second's optical axis rotated 90 degrees with respect to the first's. Then vertically polarized light is at the right angle to be down-converted by the first crystal and horizontally-polarized light by the second. This setup will emit four photons in total, with those emitted by the first crystal being entangled with those emitted by the second.

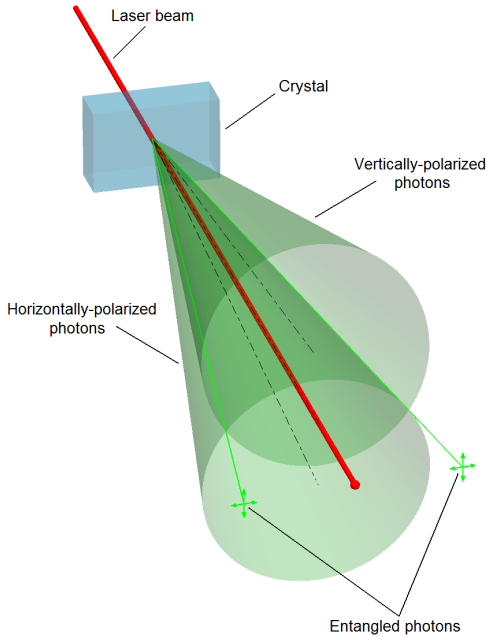

Figure 2.1.4. Emission Cones in Type-II SPDC

In Type-II SPDC, the two output beams' polarizations are perpendicular to each other as well as the input beam, and they have two distinct output cones, each with an opening angle of three degrees. These cones intersect in two places, and the detectors are placed along these paths. This means that unless we directly measure their polarizations, we won't be able to distinguish between the photons generated by the first crystal slab and those generated by the second. Equation 2.1.7, which we will recall is the mathematical expression of conservation of momentum in the y-direction, tells us that the y-components of the entangled photon pair's respective wave vectors must be equal and opposite, which implies that if a horizontally-polarized photon is detected at one of these intersections, it must have a vertically-polarized counterpart

at the other one. These photons' polarizations are intrinsically dependent on each other, which means that they must be polarization-entangled.

2.2 Demonstrating Correlation

The counts from each detector will be monitored, and a coincidence will be reported if each detector reports a photon at approximately the same time. However, not all of these coincidences will be due to entangled photons, because even with two uncorrelated beams counts are likely to coincide occasionally purely by accident. If we measure N counts in T seconds, then the average count rate would be $R = \frac{N}{T}$. If our detectors emit a pulse of width τ upon detection of a photon, then a coincidence window $\tau_c = 2\tau$ is necessary to see if the two counts overlap at all with each other. We can calculate the average count rate for each detector separately. For two uncorrelated beams, we would expect the rate of coincidences to be $R_c = \tau_c R_1 R_2$. If our experimental R_c is greater than this, we have demonstrated a correlation between the photon arrival times in the two beams and thus shown that some of them must have been generated at the same time, which means down-conversion must be happening properly.

A useful parameter for quantifying the severity of the correlation is the 'anticorrelation parameter' $a = \frac{P_c}{P_acc}$, where P_c is the experimentally-derived probability of detecting a coincidence and P_{acc} is the probability of detecting an accidental coincidence, which can also be described as the probability of detecting a coincidence between two uncorrelated beams. In general, assuming all possible outcomes of an event are equally likely, the probability of an event a occurring is $P(a) = \frac{N_a}{N_p}$, where N_a is the number of outcomes in which event a occurs and N_p is the total number of possible outcomes. Then $P_{acc} = P_1 P_2$, and $P_c = \frac{N_c}{N_p} = \frac{N_c \tau_c}{T}$ where $N_c =$ the number of coincidences measured over a time period T and $N_p = T/\tau_c$. Similarly, $P_1 = \frac{N_1 \tau_c}{T}$ and $P_2 = \frac{N_2 \tau_c}{T}$. Combining all of these, we find that the anticorrelation parameter $a = \frac{N_c}{N_1 N_2 \tau_c} = \frac{R_c}{R_{acc}}$. If there is no correlation between the two beams, $a = 1$. If the beams are well correlated, $a >> 1$. If it were possible to eliminate accidental coincidences altogether, a would approach infinity.

3
Experimental Procedure

In the full experimental setup in Fig 3.1.2., laser emits 405nm pump photons, which either pass right through the crystal along the dashed blue path or get absorbed by it and cause it to emit two 810nm photons along the light blue paths. Detectors pick up the beams and emit a pulse each time a photon hits them, and these pulses are counted up and analyzed. During the process of setting everything up, we used a red laser for alignment as shown in Fig 3.1.1 below.

3.1 Setting Up the Optical Table

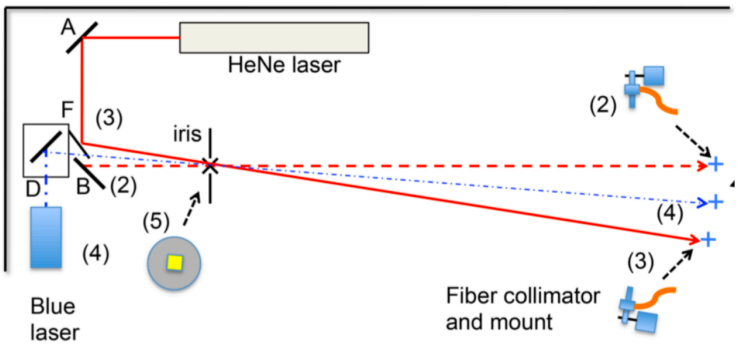

Figure 3.1.1.

First, the alignment (HeNe) laser and mirror A were placed. Mirror A was aligned so that the beam traveled parallel to the vertical edge of the optical table with the use of an iris and a

recursive method of adjusting the iris placement and the mirror angle until everything lined up consistently. Then mirror B was added and adjusted so that the beam was aligned perpendicular to its previous direction (so that it now follows the dashed red line on Figure 3.1.1). An iris was fixed in place along the beam's path in the place where the crystal will be in order to ensure that all the beams will be in the right position to pass properly through the crystal. A meter was measured down from the iris and marked as the location for the first detector above. Given that the generated particles are emitted 3 degrees from normal to either side, we know collector 2 must be 6 degrees away from collector 1 on a circle of radius 1m centered at the iris/crystal. Because the angle is so small, the horizontal change in position is very small and we can approximate the system as a right triangle with vertices at the iris and the two detectors and an angle of 6 degrees at the iris. Then the 'vertical' distance between the detectors is tan(6)=10.51 cm. Using the Pythagorean theorem we find that the hypotenuse of this right triangle is 1.0055 meters, only half a centimeter from the desired length of the beam's path, so our approximation is reasonable. Using these guidelines, a rough position for the second detector was marked, and for alignment a mirror was placed in front of the detector on its mount. Flipper mirror F was placed such that when it was in place, it diverted the alignment beam through the iris/crystal, but it could be flipped back out of the alignment beam's path. The flipper mirror and the mirror in front of collector 2 were adjusted so that after passing through the iris, the alignment beam would travel to the second mirror and reflect directly back into the iris. Then when the detector mirror was removed, the filters and collimator that make up the detector should have their faces perpendicular to the down-converted photon beam, which will help preserve more photons and keep the count rate higher.

Optical fibers were attached to the collimators on each of the collectors. Still using the alignment beam, first without the flipper mirror and then with it, the position and angle of each collector was manually adjusted to roughly maximize transmission by observing the beam intensity leaving the fiber. The path for the 405nm pump beam (dashed blue line on both diagrams) was marked halfway in between the two collectors and the laser was added so that its beam

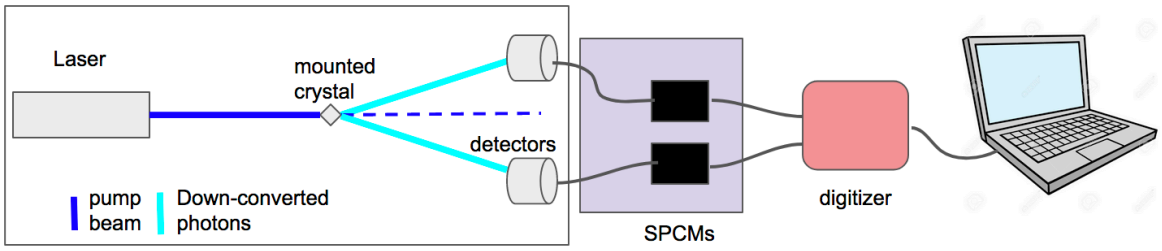

Figure 3.1.2. final experimental setup

traveled through the central iris and hit the marker indicating the proper beam trajectory. The flipper mirror had to be removed at this stage to make room for the blue laser to be secured to the optical table. The crystal was placed in a rotation mount allowing for rotation about the x-axis, and placed on a rotating stage allowing for rotation about the z-axis. The optical fibers were connected to the SPCMs, which were hooked up to channels 0 and 1 on the digitizer. The next steps would be to put the crystal in where the iris was and to perform fine alignment by adjusting the crystal's positioning and then adjusting one or both of the collectors while observing the changes in count rate, which would be recorded by the digitizer and displayed in real-time as a histogram of counts per unit time on the computer. Once the channels appear to be independently maximized, finer tuning can be done by turning on the digitizer's coincidence mode and adjusting the detectors to maximize coincidences between both channels and thus maximize the collection not just of photons in general but of the entangled photon pairs.

The collection components consist of a band-pass filter(?) to reduce ambient light noise and a collimator to gather and align incoming photons attached to a fiber optic cable which carries the photons to a single photon counting module, which emits an analog pulse when a photon enters it. The SPCMs and extra fiber optic cabling were wrapped in blackout fabric to further reduce ambient light noise that could pollute the count. Then the analog signal is transmitted to the digitizer, which is programmed to trigger when a pulse is detected, and it records the time stamp, count, and pulse shape digitally. It can also be programmed to count coincidences

on-board. This data is sent to a computer, where one can download and analyze the raw data independently, or employ the digitizer's pulse analysis software.

3.2 The Crystal

We used a Beta Barium Borate (BBO) crystal, a nonlinear birefringent crystal commonly used for this application. As outlined in the section 2.1.4, the index of refraction experienced by a photon propagating through the crystal depends on its polarization and direction of propagation, which allows us to adjust the crystal position to tailor the indices of refraction and thus the beam paths to our needs. The crystal was cut to be 0.5mm thick and mounted with the optical axis at a 30 angle such that when we shoot a stream of photons of the right wavelength (405 nm) at it, the crystal will absorb some of the photons and then release the excess energy by generating a pair of identical, position-entangled photons for each photon it absorbs at an angle of 3 degrees from normal. The entangled photon beams emerge from the crystal three degrees from normal. The vast majority of the pump photons will pass straight through the crystal unchanged, but with so many photons passing through the crystal (we have a 50mW laser which means it emits 0.05J/S of energy. The energy of each 405-nm photon is $E = hc/\lambda = \frac{6.6*10^{-35}*3*10^{8}}{4.1*10^{-7}} = 4.8 * 10^{-20}$, so the number of photons the laser pumps per second is $\frac{0.05}{4.8*10^{-20}} \approx 10^{18}$, or about one quintillion!) the small percentage of these that do become absorbed and emitted will still amount to a significant number of generated entangled photon pairs.

Because of conservation of energy, we know the sum of the energies of the two generated particles must be equal to the energy of the input particle; recall that photon energy is inversely proportional to wavelength, so our generated photons will be at 810 nm. The top end of the visible spectrum is red light at 740nm, so the generated photons are not visible at all (at least with our feeble human eyes). This can be dangerous as one can't immediately tell where the beam is pointing, and direct exposure to a sufficiently strong laser beam at any frequency can be hazardous.

The photon pairs emitted by one crystal are energy-entangled, but not polarization-entangled as they will always have the same polarization, informed by the orientation of the crystal. In order to produce polarization-entangled photons, we adhere two of the very thin slices of crystal together, with one rotated 90 degrees from the other. Then the pairs generated by the first crystal will be vertically polarized while the pairs generated by the second will be horizontally polarized. The pairs generated by each crystal radiate out from it in three-degree cones that diverge from each other. The two cones intersect along two paths, and by setting up our collectors at these points, we are introducing uncertainty about which photons were generated by which crystal, because besides the polarization they are otherwise indistinguishable. Then when we detect a photon at each of the collectors at the same time, we don't know which one came from which crystal, but we do know that one came from one crystal and one from the other, and so their polarizations must be opposite- one is horizontally polarized and one is vertically polarized. Before we measure either photon's polarization, it does not have a definite value. Once we measure one and it picks a value, we know with certainty that the photon we have not measured must have the complementary polarization, and thus the two are necessarily entangled. Of course each crystal is still generating pairs of photons, so in the end we wind up with four photons, where the two from the same crystal are position-entangled and each one from one crystal is polarization-entangled with both photons from the other crystal.

3.3 Coincidence Counting

The entangled photons are generated at the same time and with the same frequency and complementary momenta, which means they should reach the detectors at the same time; we look for entangled photons by examining instances in which both detectors trigger at the same time. The pulse emitted by the SPCM has an experimentally-derived duration of about 10ns, which limits how precisely event times can be recorded. This means that when we're looking for 'simultaneous' events, the best we can do is look for instances where the actual pulses overlap, or where an event is triggered on one detector within a certain amount of time, called a coincidence window,

of an event triggering on the other detector. Even with completely random and uncorrelated beams, as long as enough photons pass through there will be times when photons happen to simultaneously reach the detector by chance. The average number of accidental coincidences can be predicted based on the count rate and the coincidence window (see section 2.2), and observing a significantly higher coincidence rate between the two beams than this prediction demonstrates a correlation between the beams and confirms the presence of entangled photon pairs.

A larger coincidence window would cause a dramatic increase in the number of accidental coincidences reported, but while a smaller coincidence window would minimize the accidental coincidences, it would also increase the likelihood that true coincidences due to entanglement are not reported, because there are other factors that may cause a temporal offset between photon arrivals, such as discrepancies in the distance traveled in the optical and coaxial cables. Too high of an intensity of the input beam would result in a higher count rate, which increases the risk of overloading the photodetectors and causing them to operate imperfectly for quite some time. Besides that, a higher count rate means less time in between events, which can also cause issues for the photodetector due to its method of operation.

3.3.1 Single Photon Counting Modules

We used Excelitas' Single Photon Counting Module SPCM-AQRH. The SPCM contains an avalanche photodiode, wherein an incoming photon will knock an electron out of place and that electron displaces other electrons in a chain reaction. This causes an electron 'avalanche', which builds up a noticeable voltage difference across the detector and sends an analog pulse to the digitizer. After this cascade of electrons, it takes some time for the charge to dissipate as the electrons spread back out. This is called dead time. If a photon enters the photodiode before the electrons have gone back to their normal distribution, it may not be able to trigger a big enough electron cascade to meet the voltage threshold, and it will not only not produce a consistent pulse but it will reset the dead time, which is up to 25 ns according to Excelitas. If too much light enters the module over some length of time, it can oversaturate the detector and cause it to misbehave for up to an hour.

In order to get the digitizer to reliably trigger a count based on the signal, it was important to understand the nature of the SPCM's output pulses. To do this, the SPCM was placed in a dark room and hooked up to an oscilloscope, allowing us to examine the pulse shape. Originally, the pulse looked like a damped oscillator, indicating that the signal was reverberating. A 50-ohm terminator was added before the oscilloscope and the reverberations ceased, leaving a signal that was not a square wave but was a wide and squat curve with a width of approximately 10 ns that appeared to be consistent from pulse to pulse. The digitizer accepts analog signals up to 2.0 V or can be set to a 0.5V scale. Being able to use the 0.5V setting allows for greater resolution when reading the signal, and the SPCM pulse was already uncomfortably close to the 2V limit, so a 20 dB attenuator was added as well to reduce the SPCM pulse voltage. This was done successfully without altering the signal shape.

3.4 Digital Data Acquisition System

3.4.1 Digitizer Hardware and Firmware

We used the CAEN Group's DT5725 desktop digitizer with DPP-PSD firmware. The digitizer's primary function is digital pulse processing (DPP), meaning it converts the analog signal to a digital one and records the shape of the signal, either on a 2.0 or 0.5-Volt scale. By making the signal digital, we are changing a continuous wave into an approximation based on a finite set of data points. This inherently results in a loss of data but we can attempt to minimize it. The digitizer takes the signal and makes it discrete by dividing the continuous range of possible voltages into many small voltage steps and records the signal based on how many steps need to be stacked up to reach the voltage of the input signal. Our digitizer is 14-bit, which means it divides the voltage range up into 2^14 steps. Because the device can only take 2^14 data points regardless of voltage scale, if we can use the 0.5V scale instead of the 2V scale, the density of data points per volt will quadruple and greater signal resolution will be retained. The smallest voltage increment is called the Least Significant Bit, or LSB, and is the unit used for adjusting all voltage-related settings on the device. According to the manufacturer, one LSB equals 0.12mV

on the 2V scale and 0.03mV on the 0.5V scale. This is easily confirmed by dividing the total voltage window, which is either 2 or 0.5, by the number of bins, which is 2^14 or 16,384, and it helps demonstrate how using the 0.5V scale retains more precise information. In our case, we are looking for pulses and we are not concerned so much with the shape of the signal, so this isn't a large concern. In theory it could increase the accuracy of the pulse timing, but that is already limited by the 4ns resolution of the digitizer's time stamps.

The device also has different options for triggering, recording, and analyzing the signal on-board which can be set to suit the user's needs with respect to data collection and analysis. The digitizer came with firmware and computer software for changing its settings and for data analysis suited to some of the digtizer's main uses, such as event counting and pulse analysis. We used their pulse shape discrimination (DPP-PSD) software and firmware. Different functions also allowed for the user to communicate with the digitizer at different sort of levels of abstraction. One very useful feature of this digitizer is that it has a field programmable gate array (FPGA), which can be set to perform different basic logical operations between pairs of channels. By turning on the digitizer's coincidence mode, we tell the FPGA to become an AND gate. When an event is occurring on one channel, it sends a signal to the FPGA and the corresponding input becomes true. Most of the time, either both inputs will be false or one will be false and the other one true, in which case the logical AND of the inputs is false. But if there's a moment of overlap between the events on the two channels, then both inputs will be true and the FPGA will relay the signal. By adjusting the length of the event to fit the width of our input pulses, we can have the digitizer pick out the coincidence counts on-board.

At its heart, the digitizer has saved a bunch of groups of numbers that tell it what to do. The groups are called registers, and our digitizer has hundreds of 32-bit registers that can be accessed by the user. All computer function boils down to binary (counting in base 2, every digit is either 0 or 1, yes or no, signal or no signal, etc), and a 32-bit register corresponds to a 32-digit binary number. However, working with that many digits can quickly become unwieldy, and although at the technical level all digital operations are necessarily binary, the registers

are read and modified by the user in hexadecimal (base 16), which requires only eight digits to convey the full 32 bits of information. Even though the string of digits that makes up a register can look like one big number, in many cases different chunks of it mean different things. For example, each of the eight channels has a register at address 0x1n80 where n is the channel number for DPP Algorithm control. The arrangement of the first three bits tells the digitizer which one of twelve possible settings for charge sensitivity to employ. Besides these first bits and bits 18 through 22, every other bit in this register turns on or off a different setting for the data collection. Some registers, on the other hand, are dedicated to one more complex feature, or are used to store information necessary to the digitizer's operating procedure that is not related to user input and thus is not explained in the manual and cannot be changed by the user. For example, the threshold over which the digitizer will trigger an event on a channel n can be set at many different levels, so in order to know what to do the digitizer requires more information than a simple one-bit 'on' or 'off', and as such it requires more digits to convey that information. In order to adjust the trigger threshold directly via the registers, the user must change the first fourteen bits of register 0x1n60, while its remaining bits are reserved for other functions and cannot be written over by the user. The digitizer comes with a list of all the user-accessible registers, some of which can be altered by the user, but there are many more that we cannot (and have no reason to) access.

3.4.2 Digitizer Software

Reading and writing to the registers in hexadecimal is the most fundamental level on which one can communicate with the digitizer. The user downloads a software driver and a series of libraries of C functions that allow the computer to communicate with the device. One can make their own java programs using these functions, or put them together in Labview, but the higher-level libraries also come with a pre-made user interface called CAENComm Demo as both a Java and a Labview file. This demo is very basic- it allows the user to establish a connection to the digitizer, and to directly read and write to the available registers. It does not allow one to record or save pulse data. It is mostly helpful for debugging and for verifying that the computer and

the digitizer are communicating correctly. I briefly used this demo to establish a connection to the digitizer and to mess around with the read and write functions to help me understand how the registers worked.

Figure 3.4.1. A screenshot of the CAENComm graphical user interface.

The DPP-PSD control software is the lower-level interface that allows for data acquisition. It is similar to the CAENComm Demo, but includes a basic oscilloscope and can perform data acquisition (either as the raw hexadecimal output or as a histogram of counts per second or pulse energy). It includes a tab for monitoring the device temperature and performing calibration and a tab for choosing active channels. I used this program to check how long the digitizer temperature fluctuates after being turned on (calibration is done automatically upon connection to the digitizer, but to ensure accurate readings it should be repeated once the digitizer reaches its operating temperature which I found to be at around 40 degrees celsius). I also used this software when doing preliminary checks of the count acquisition system. I had an SPCM wrapped in blackout fabric hooked up to the digitizer and I used the software's oscilloscope to observe the counts and note the pulses' characteristics as they passed to the digitizer. I had the digitizer record some of this dummy data on the computer to familiarize myself with the digitizer's raw output format, which consists of four 32-bit header words followed by any additional data which can vary based on setting. The four header words include a flag to indicate board hardware issues and information about the event size and format, the type of trigger, the participating channels,

the total event count, and the time at which the event was triggered. The only data we need from this is the trigger time tag. I had been having difficulty with the digitizer's LabView program and so at this time I was trying to understand the raw data output so that I might be able to write a Matlab program to read the time tags from the data file and search for coincidences.

The DPP-PSD control software does not have a function for reading and writing to the registers in real time, and any changes the user makes to the digitizer settings must be done in hexadecimal in the DPP-PSD control software's configuration text file. While attempting to familiarize myself with this software, I successfully edited the configuration file to turn on and off coincidence mode and to change the voltage scale. However, with the exception of the voltage scale change which is immediately apparent on the oscilloscope tab, I would have to open the CAENComm demo and read the relevant register every time I wanted to confirm the current setting of one of the parameters, and I'd have to edit and save the configuration file and reload everything to make any modifications. While this program was very helpful in understanding the way the digitizer functions and doing preliminary signal checks, it is not very convenient for making quick adjustments during the collection process and is not the software we have employed for the actual data acquisition.

The program we ultimately used for data acquisition, which is designed for higher-level digitizer manipulation and data acquisition, is CAEN's CoMPASS (Caen Multi-PArameter Spectroscopy Software) program. This program has a function for directly reading and writing to the registers, but it also has more user-friendly interface that allows the user to make adjustments to the data collection parameters on each channel without having to look up which register the information is stored in and write to it directly. For example, let's say I want to change the voltage threshold above which the digitizer will trigger an event for channel 0. I could access register 0x1060 and write the hex value for how many LSB I'd like the threshold to be in its first fourteen bits, but there is a tab on the CoMPASS interface where I can enter the new threshold in regular old base-ten and the software will convert to hexadecimal and write to the

correct register for me. This saves a lot of time and allows the user to check or edit the current configuration of lots of the parameters at once.

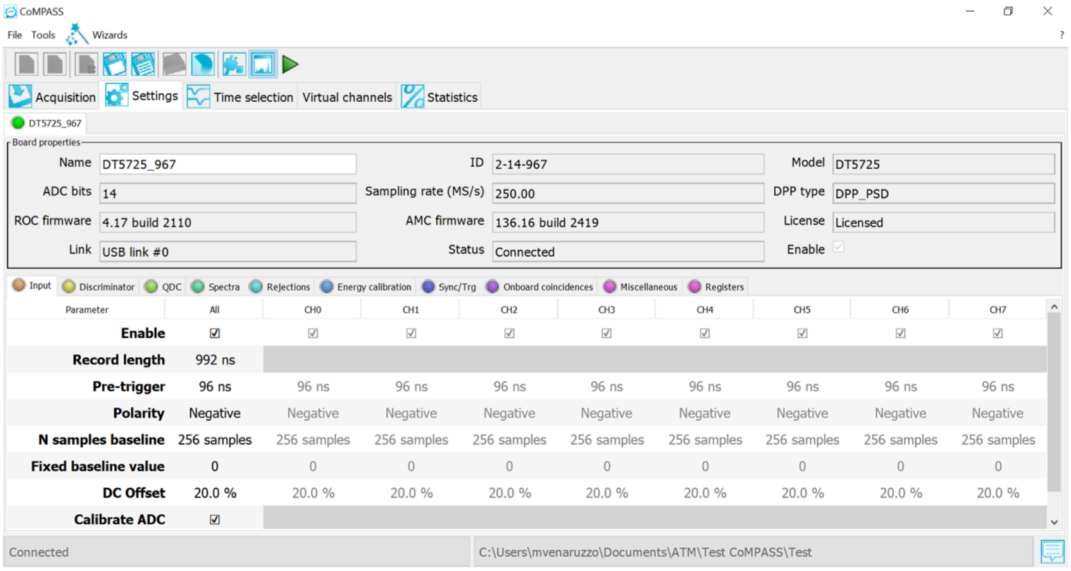

Figure 3.4.2. A screenshot of the Settings tab of the CoMPASS software

Once the user has opened the CoMPASS software and established a connection to the digitizer, the program will open to the Acquisition tab. Here one can start or stop data acquisition and choose what parts of the data (such as pulse energy, wave form, trigger timing, and various spectra) should be saved and exported. One can opt to filter out events that are flagged as pileup events, which can occur when the count rate is too high, and oversaturation events, which happen when the signal voltage exceeds the voltage scale. The user can choose to further filter out rejected events, which are flagged because they are the wrong size or shape. Setting up parameters for event rejection is more important situations requiring careful discrimination of the pulse shape, like when trying to discern between different incoming wave forms, and is not so applicable to our circumstance. Like the DPP-PSD control software, the user can set up a configuration file to choose the settings under which the digitizer will be opened, but barring some need for special operations that can't be controlled through the CoMPASS interface, it is not necessary.

The second tab is the settings tab. It has several subtabs and it is where the user sets all the parameters for each channel. Of all of these, only some were relevant to our situation and of the ones that were relevant, only a few had to be adjusted to suit our needs. In the input subtab, we set the length of the acquisition window, shortened the pre-trigger (which sets how many nanoseconds of waveform are saved prior to the event trigger) because we are not concerned about pulse shape, ensured that the pulse polarity was set to positive and the Analog to Digital Converters were set to calibrate at the beginning of every run, and changed the voltage scale to 0.5V. Under the discriminator subtab, we chose the discriminator mode to be leading edge (meaning that an event is triggered as soon as the signal passes the voltage threshold), set the threshold in LSB relative to the calculated baseline, and set the trigger holdoff (the amount of time that must pass after an event is triggered on a channel before another event can be triggered on that channel) to be 24ns given the 10ns pulse width and the digitizer's timing resolution. Under the Onboard Coincidences subtab, we enabled coincidence mode as "Ch0 AND any' so that all other channels would only record events when they triggered within the coincidence window of one of Channel 0's events, and we set the coincidence window to about 24ns. Under the QDC subtab, we set the gate to approximately 40ns. The rest of the QDC subtab and the remaining subtabs were not adjusted. Many of the settings which required a numeric value would only accept multiples of four or sixteen, but when the user enters a value that is not supported, CoMPASS notifies them and sets the parameter to the nearest acceptable value. All acceptable values for each parameter can be found either in the CoMPASS User Manual or the DT5725/DT5730 DPP-PSD Register Description.

The other useful tab is the Statistics tab. It shows how frequently different signals are passing through the eight channels, including the total throughput for each channel as well as the input count rate or ICR (which is the raw number of events being sent into the digitizer), the output count rate or OCR (the number of events that are included in the final data), and the rate of incoming saturation, pileup, and rejected events. This page is useful for alignment and for troubleshooting. In general the ICR should equal the sum of the OCR and the various rejection

rates, so by looking at the statistics tab we can get a good idea of how many pulses per unit time are being sent from the SPCM, what proportion of those are making it through to the final tally, and why the ones that don't make it through are being rejected.

4
Future Steps

Unfortunately, at the time when the lab was closed to the public, we had just installed the pump laser and mounted the crystal and were about to add the crystal to the optical table and do the fine alignment of the detectors as outlined in section 3.1. This is the immediate next step, followed by demonstrating correlation between the beams. Then, though, the fun stuff begins as we get to play with the entangled photons and do various experiments that demonstrate the quantum nature of light. One such experiment is the John Wheeler's Delayed-Choice Experiment, which focuses on the wave-particle duality of light.

4.1 Wave or Particle?

As we know, light can behave as a wave or as a particle, depending on the physical situation. We can know definitively that a photon is behaving like a particle by finding its exact position, which would not be a physical reality if the photon was a wave, and we can know the photon is behaving like a wave if we can get an interference pattern from it. A wave necessarily has an amplitude of some kind that oscillates up and down. Then when two light waves come together, they combine into one wave that's shaped at each point on the curve by the sum of the two input waves' amplitudes. If the waves have the same frequency and are perfectly in phase, their amplitudes will peak and bottom out in the same places, and so the resultant wave will have the

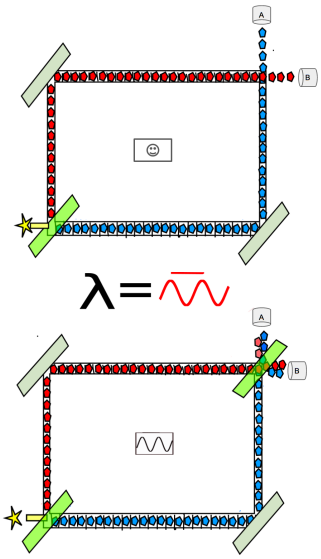

Figure 4.1.1. In the top setup, the photons exhibit particle-like behavior. When we add a second waveplate and obtain the bottom setup, the photons exhibit wave-like behavior.

same frequency and double the amplitude at every point. This is called constructive interference. When there's a 180 degree phase shift between the waves, one's peaks line up perfectly with the other one's troughs and vice versa so that the waves cancel each other out. This is called destructive interference. A simple set-up for demonstrating how one can probe the photon's wave- or particle- like nature involves modifying a basic Mach-Zehnder interferometer. In the below figure, the green blocks are 50/50 beam splitters and the gray blocks are regular mirrors. In both cases the photon enters the from the bottom left and at the top right we have two detectors facing the top left corner of the interferometer, one from above (detector A) and one from the left (detector B). The beam splitters introduce uncertainty about the photon path- each input photon that interacts with the beam splitter on the lower left has an equal chance of being transmitted to the mirror on the bottom right (following the blue path) or being reflected to the mirror on the top left (following the red path).

In the top set-up, after the beam splitter each path heads to the top right corner. When we try to detect these photons at the top corner, we know that any photons registered by Detector B must have taken the red path and those that are registered by Detector A must have taken the blue path. Then because light has a constant velocity, given that we know the time at which

a photon reaches a detector and the path it must have taken, we can work backward and know with certainty exactly where each photon was in the path as a function of time. Then because we can point to a definite position of the photon, we know it must be behaving like a particle and not a wave.

In the bottom setup, we add another beam splitter at the top right corner. Then when an incoming photon coming from either path enters the new beam splitter, it has a 50/50 chance of propagating toward each detector- Detector A will register the reflected red-path photons and the transmitted blue-path photons, while Detector B will register the transmitted red-path photons and the reflected blue-path photons. The new beam splitter recombines the two paths, so that now we can't differentiate between red-path and blue-path photons because both are going to both detectors and are otherwise indistinguishable. Now when we look at the pattern recorded by each detector, it will not show a bunch of temporally distinct, particle-like behavior- instead it will show an interference pattern informed by the phase shift experienced between the two photons, which depends on how many times and where each wave was reflected/transmitted. Based on the data we receive from the detectors we can figure out either the photon's definite position as it travels through the interferometer or we can figure out its definite phase and frequency. Then even though the set-ups are identical prior to the beam splitter position, in one case we can know wave-like information about the photon as it travels through this region and in the other we can know particle-like information.

This behavior is pretty strange to us. It seems almost as if the photon must be looking ahead at what's going to happen to it and deciding how to act based on the circumstances under which it will eventually be detected! It raises questions for us (or at least, for me) that are very similar to the ones that Wheeler was grappling with when devising his delayed-choice experiment: Is there something in this experiment that we're missing? Are we right in concluding that the photon's state inside the interferometer can be extrapolated based on how we measure it when it leaves? Is a photon somehow capable of making the 'choice' to behave as a wave or as a particle? How can it make the right choice every time it enters the set up unless it has some awareness of what

is waiting for it at the end? How is it possible for a photon to appear to be so conscious of itself and its surroundings? At what point does the 'choosing' happen and the photon's state becomes definitely one or the other? It turns out that things only get weirder from here. The following outlines a modified delayed-choice experiment that employs the energy-entangled photon streams we will have generated via the Type-II SPDC procedure outlined above.

4.2 An Illuminating Experiment

4.2.1 Wave Packets and Coherence Length

Although we have been referring to the pump beam's wavelength as exactly 410nm, in reality 410nm is the average frequency- the beam contains light waves along a range of frequencies called the bandwidth ($\Delta\lambda$), which means the down-converted photons do as well. When light waves of many frequencies within a small range are added together, as they do in the pump beam, they tend to destructively interfere except for a small range in which they interfere constructively. This results in a localized bump that propagates through space called a wave packet. Taking the Fourier transform of the wave packet will break it back up into a sum of its constituent frequencies. The length of this packet is called the coherence length ℓ_c and is dependent upon the beam's bandwidth and average frequency according to the relation

$$\ell_c = \frac{\lambda^2}{\Delta\lambda} \tag{4.2.1}$$

.When a beam like this is split into two paths and later recombined, sometimes one path can be longer than the other, meaning the signal from that path will take longer than the other to reach the point where they are recombined. The two recombined beams can only interfere with each other if the difference in their arrival times- and thus the difference in their path lengths ΔL- is small enough that some portion of the wave packets overlap. Then in order to see interference between the two beams, the difference in path lengths and the input beam's bandwidth must satisfy the relation

$$\Delta L < \ell_c \tag{4.2.2}$$

Because light's energy is proportional to its frequency, the uncertainty in the down-converted photons' frequency translates to uncertainty in their energy, and therefore both photons' wave functions must be a superposition of multiple energy eigenvectors informed by the beam's bandwidth. Then because our photons are energy-entangled, changing the bandwidth of one photon will change the bandwidth of the other.

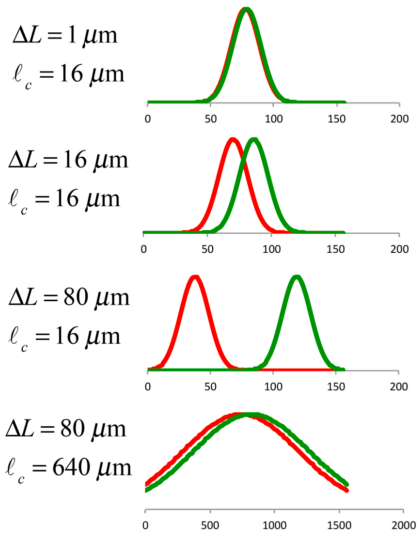

Figure 4.2.1. The pulses overlap and fully interfere when $\Delta L < \ell_c$. When $\Delta L \approx \ell_c$, like in the secondd graph, there is partial interference.

4.2.2 Putting it All Together

Setting up the optical table for this experiment entails setting up a Mach-Zehnder interferometer in one of the down-converted beams' path. One of the interferometer mirrors will be mounted on a piezoelectric translation stage so that its position can be reliably adjusted on a nanometer scale. This will be used to tune the difference in path length between the two arms of the interferometer. After exiting the interferometer, photons on path B pass through a band-pass filter and into detector B. The photons on path A are collected and sent through a 20m fiber before being spit back out into the open air and passing through another band-pass filter to detector A. 20m of coaxial cable are added between detector B's SPCM and the digitizer in

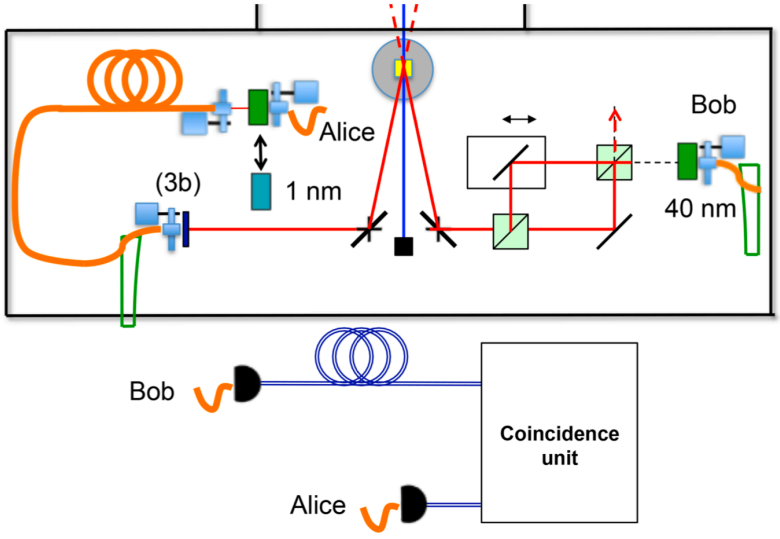

Figure 4.2.2. Additions to our experimental setup that allow the user to perform the Delayed-Choice experiment.

order to even out the lengths of paths A and B so that pairs of entangled photons will still arrive at the digitizer at roughly the same time and trigger a coincidence count.

From equation 4.2.1 we can see that the coherence length of a wave packet increases as the bandwidth decreases. Then when we pass photon A through a filter to decrease its bandwidth, photon B's bandwidth follows suit and its coherence length increases. By setting ΔL so that it is less than the modified coherence length but greater than the original, undisturbed coherence length, we can see exactly when photon B's bandwidth changes by noting when we start to see interference in the interferometer, and see how its timing relates to the time at which Photon A passes through the filter! In order to achieve this, we put both beams through a wider band-pass filter and adjust the position of the piezo away from perfect alignment (increasing ΔL) until we just reach the point where there is no longer interference between the two interferometer arms. Then we examine the interference, switch out the filter before detector A with a filter with a smaller bandwidth, and see how path B's interference pattern changes. We find that when detector A's filter (with which we aligned the interferometer such that the light travelling through its didn't quite manage to interfere) is replaced by a filter with a smaller bandwidth, we start to see an interference pattern at detector B.

But you may be asking, what's with the extra 20m of cabling? This is where the "delayed" part of the experiment name comes from, and it's where things get really mind-boggling. It takes some time for the signals to travel through the extra length of cabling. This means that while photon A is still moving through the fiber optic cable, photon B has already passed through the interferometer and entered detector B. At this moment, photon B has already interfered with itself and therefore the level of interference that is detected by channel B ought to be set, but photon A still has yet to pass through its filter. That all seems well and good until we remember that detector B's filter is what dictates the coherence length of both beams. We consistently see interference in photon B when the smaller bandwidth filter is in place and see no interference when the wider filter is in place, even though the amount of interference present is recorded before photon A even reaches the all-important filter. This shows that we can delay the choice of bandwidth (and thus coherence length) until after the photon has already passed through the interferometer without changing the outcome!

Without getting into the mathematical formulation, the wavefunction of this system is dependent upon both photons. Each photon is detected at some point and their detection collapses the system's state. However, at the end of it all, the system's wavefunction is only dependent on energy, wavelength, the filters' bandwidth, and ΔL- it is not dependent on time, and so it doesn't matter what is recorded when. Quantum mechanics' best explanation for this delayed-choice behavior is that before photon A is detected, the wavefunction includes interference information for both cases, and that by selecting the bandwidth of the filter in path B we are choosing which subset of this information to access.

Besides the procedures outlined in this thesis which attempt to probe the quantum nature of light, the phenomenon of quantum entanglement has many promising possible future applications. It is used in quantum computing to help create faster, more powerful computers. It is being examined in the field quantum cryptography as a way of generating quantum keys which cannot be intercepted by a third party and then used to decode sensitive information. It is being examined as a way to increase the precision of atomic clocks and a way to quickly communicate

across long distances. Quantum Teleportation, a process in which two entangled photons essentially 'switch places', has already been achieved with one photon on earth and the other all the way up in space. Learning how we can harness the power of quantum entanglement is leading to new practices and improvements in fields across the STEM spectrum.

Bibliography

[1] Enrique Galvez, *Correlated Photon Experiments Laboratory Manual* (2008).

[2] A. Einstein B. Podolsky and N. Rosen, *Can the Quantum-Mechanical Description of Physical Reality Be Considered Complete?*, Physical Review **47** (1935).

[3] John Bell, *On the Einstein Podolsky Rosen Paradox*, Physics Physique Fizika **1** (1964).

[4] Mark Beck, *Quantum Optics Lab Write-Ups*, 2019.

[5] CAEN Group, *Digitizer Family DT5725/730 User Manuals and Guides*, available at `https://www.caen.it/download/?filter=DT5725`.

[6] Excelitas, *SPCM-AQRH Famlily Datasheet*, available at `https://www.excelitas.com/product/spcm-aqrh`.